

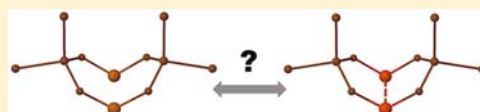
More on Diphosphadithiatetrazocines and the Importance of Being Bonded

Heiko Jacobsen*

KemKom, 1215 Ursulines Avenue, New Orleans, Louisiana, 70116, United States

S Supporting Information

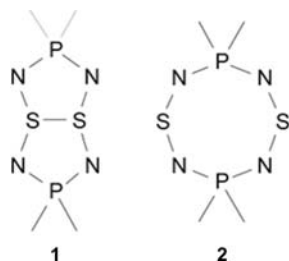
ABSTRACT: The cross-ring sulfur–sulfur bond for seven $R'RP(NSN)_2PRR'$ molecules **1a** ($R = R' = \text{Me}$), **1b** ($R = R' = \text{Ph}$), **1c** ($R = R' = \text{Et}$), **1d** ($R = \text{Cl}$, $R' = \text{CCl}_3$), **1e** ($R = R' = \text{Cl}$), **1f** ($R = R' = \text{F}$), and **1g** ($R = R' = \text{H}$) has been scrutinized by a topology analysis for a bond descriptor based on the kinetic energy density, supported by a fragment-based bond energy analysis. Contrary to a regular disulfide bond, the cross-ring connection is only a secondary electron-sharing bond, about half as strong as a common S–S linkage. The regular disulfide bond itself is best described as a charge-shift bond. These analyses are based on results obtained from B3PW91/def2-TZVP density functional calculations.



INTRODUCTION

The importance of being bonded is the title of a fairly recent commentary in which Rzepa embarks on a descent into the world of a molecule and explores the electronic phenomenon commonly known as the chemical bond.¹ His captious interrogation of the opening statement that “all chemists when asked would probably say that they ‘know a bond when they see one’” summarizes if not the nature then the crux of chemical bonding — it now seems that the chemical bond is better described as noumenon rather than as phenomenon.^{2,3}

Rzepa begins his exposition with the fundamental distinction between structure and bonding and soon arrives at the idea of aromaticity — a property that not only has sustained essential developments in organic chemistry but also has gained increased recognition in inorganic chemistry. He then chooses a variety of approaches out of the rich arsenal of methodologies available to illustrate the complexity of this topic, ranging from Lewis structures and molecular orbital approaches to density-based descriptions and spectroscopic fingerprints. His illustrations are based on one single inorganic molecule,⁴ an epitome of the group of diphosphadithiatetrazocines $1,5-R_2P(NSN)_2PR_2$ (**1**). Although initially represented as planar ring structure **2**, X-ray analysis revealed the folded structure **1**, which implied some cross-ring sulfur–sulfur interaction.



This intriguing class of molecules not only caught Rzepa’s attention as a perfect example to illustrate a bonding conundrum but continues to challenge researchers in general

— not too long ago, the bonding in diphosphadithiatetrazocines **1** received renewed attention,⁵ and Chivers and co-workers recently extended the cast of $1,5-R_2P(NSN)_2PR_2$ compounds by yet another representative ($R = \text{Cl}$).⁶ The researchers not only introduced a new member of the diphosphadithiatetrazocine family, but they also employed established computational methodologies and provided arguments that support the newly proposed bishomoaromatic character⁵ as well as the through-space bishomoconjugation in the eight-membered ring of $1,5-R_2P(NSN)_2PR_2$ molecules.

Rzepa’s point-by-point presentation makes it clear that the quest for chemical bonding strongly depends on the definition of the term itself and on the selected target group of atoms within a molecule, which might or might not be considered to engage in chemical bonding. Yet, for diphosphadithiatetrazocines **1** it was the apparent existence of a cross-ring sulfur–sulfur bond, suggested by NMR and Raman spectroscopy, and confirmed by an X-ray structural determination, that was recognized as the most exhilarating feature of this new class of compounds.⁴ Although an omnipresent structural motif, the disulfide linkage itself is rather flexible and not easily classified by a characteristic sulfur–sulfur bond energy; combining experimental and theoretical results, Denk recently established a disulfide bond-strength range from 170 up to 330 kJ/mol.⁷

Thus, the question whether the transannular S–S interaction classifies as a bond or even as a chemical bond constitutes the central theme of the present work. We use established as well as newly developed methodology to put this problem into proper perspective, and it is hoped that this extension of a basic theme might provide some new ideas for the resolution of some unsolved old problems.

Received: May 31, 2013

Published: October 1, 2013

■ BACKGROUND

Before we proceed with a discussion of our results, we set the stage and present some essentials of the selected class of molecules and of the chosen methods of bond analysis. The reader who is familiar with $R_2P(NSN)_2PR_2$ molecules, with bond descriptors based on the kinetic energy density, and with fragment-based bond energy analyses, might want to skip to the end of the corresponding sections.

On Diphosphadithiatetrazocines. Diphosphadithiatetrazocines $R_2P(NSN)_2PR_2$ are eight-membered rings that may be envisioned as amalgam of the archetypical cage-compound S_4N_4 and monocyclic cyclotetraphosphazenes $(R_2PN)_4$.⁶ The first representative, 1,5- $(CH_3)_2P(NSN)_2P(CH_3)_2$ **1a**, was isolated and characterized in 1982 as decomposition product of the six-membered ring $(Me_2PN)(SN)_2$, which in turn was obtained when reacting the cage molecule S_4N_4 with Me_2PPMe_2 .⁴ Although initially envisioned as an inorganic example of an aromatic ring system, a crystal structure determination revealed its folded arrangement. Shortly after, the solid state structure of a second specimen of this new class of compounds, 1,5- $(C_6H_5)_2P(NSN)_2P(C_6H_5)_2$ **1b**, was reported.⁸ As a consequence of their folded bicyclic ring-structure, derivatives of diphosphadithiatetrazocines, in which the two substituents on phosphorus differ, form various structural isomers, and improved syntheses for molecules of the type 1,5- $RR'P(NSN)_2PR'R$ led to the crystal structure determination of two more representatives with $R = R' = Et$ **1c** and $R = Cl, R' = CCl_3$ **1d**.⁹ Although by now well-established, the extension of the family of diphosphadithiatetrazocines molecules, such as $Cl_2P(NSN)_2PCL_2$ **1e**,⁶ and an exploration of their underlying bonding motifs^{5,6} continue to receive well-deserved attention.

On Kinetic Energy Density Descriptions of Chemical Bonding. The richness in bonding is one of the reasons why a chemical bond is not as clearly defined as one would wish, but if a chemist were asked to name the quintessential chemical bond, the answer would most likely point to the covalent bond. A covalent bond results from electron sharing between two or more atomic centers, and the driving force of covalent bonding is a lowering of the quantum kinetic energy density.¹⁰ Thus, concepts built on the kinetic energy density appear to be most appropriate for an analysis of chemical bonding. One such function that is based on local kinetic energy densities and that evaluates their chemical content became known as localized orbital locator $\nu(\mathbf{r})$.¹¹ The kinetic energy density of electrons within a molecule $\tau(\mathbf{r})$ is put in relation to that of the uniform electron gas $\tau_0(\mathbf{r})$, and the function $\nu(\mathbf{r})$ maps values of the ratio $\tau_0(\mathbf{r})/\tau(\mathbf{r})$ onto the finite range $0 \leq \nu(\mathbf{r}) \leq 1$. A $\nu(\mathbf{r})$ -value of $1/2$ corresponds to regions where the local kinetic energy of the electrons resembles that of the uniform electron gas, whereas regions with larger $\nu(\mathbf{r})$ -values are characterized by relatively slow moving electrons. This then implies a reduction in kinetic energy density and might be interpreted as indicative of covalent bonding.

The function $\nu(\mathbf{r})$ has been successfully used in the characterization of prototypical¹² as well as atypical¹³ chemical bonds and continues to receive increased recognition as a valuable approach to bond analysis.¹⁴ Furthermore, a gradient path analysis of the scalar field of $\nu(\mathbf{r})$, which classifies as a quantum chemical topology (QCT) approach,¹⁵ reveals distinct patterns that can be related to particular aspects of chemical bonding.¹⁶ Bader has pioneered QCT for the charge density

$\rho(\mathbf{r})$ as a function of interest, culminating in the theory of *Atoms in Molecules* (AIM),¹⁷ but shifting the emphasis onto the kinetic energy density leads to a fundamentally different description of chemical bonding: while methods based on $\rho(\mathbf{r})$ deduce the presence of a chemical bond from answers to the question where electrons *are*, $\nu(\mathbf{r})$ methodologies are based on answers to the question where electrons *stay*.

On Fragment-Based Bond Energy Analyses. The idea that a chemical bond results from the electronic interaction of certain fragments is intuitively clear to chemists, but it inherently incorporates some bias, since the selection of suitable fragments is not unique. Hence we briefly outline our chosen approach of bond fragmentation.

The primary contribution to the energy of a chemical bond within a molecule arises from the interaction of two fragments that both possess the local equilibrium geometry of the final molecule and that both have an electronic structure suitable for bond formation; the energy associated with such a process is referred to as bond snapping energy BE_{snap} .¹⁸ The bond energy BE is obtained when the bond snapping energy BE_{snap} is adjusted by the so-called preparation energy ΔE_{prep} , that is, $BE = BE_{\text{snap}} - \Delta E_{\text{prep}}$. Here, ΔE_{prep} summarizes the energy required to set up the fragment for bond formation; it involves the deformation energy when the optimized ligand framework adopts the geometry of the final molecule, and, if required, the promotion energy from the electronic ground state of the fragment to the electronic valence configuration suitable for bond formation.

To reiterate, the scheme presented here shares with other methods of analysis a certain degree of arbitrariness, since the bonding picture that it provides depends on the choice of fragments used to describe the formation of a resulting entity. But what appears as weakness might be also seen as strength since it calls for and allows the use of elementary ideas and patterns a chemist is familiar with. For the interested reader, we refer to a recent paper, in which further aspects of fragment-based bond analyses are elucidated, and unification of charge and energy decomposition schemes for bond analyses is achieved.¹⁹

■ RESULTS AND DISCUSSION

The folded arrangements of the seven $R'RP(NSN)_2PRR'$ molecules **1a** ($R = R' = Me$), **1b** ($R = R' = Ph$), **1c** ($R = R' = Et$), **1d** ($R = Cl, R' = CCl_3$), **1e** ($R = R' = Cl$), **1f** ($R = R' = F$), and **1g** ($R = R' = H$) constitute the core elements of the present work; the structures of compounds **1a–1d** have been determined by X-ray analysis,^{4,8,9} and **1e** represents the latest addition to the group of diphosphadithiatetrazocines.⁶ Quantum chemistry computations for the unknown fluorine analogue **1f** have already been carried out to assess the influence of electronegative substituents on the structure of the eight-membered rings,⁶ and **1g** has been added as the simplest model compound. In addition, the set of molecules has been extended to the corresponding planar dicationic ring systems $2a^{2+}-2g^{2+}$, motivated by the X-ray structure of a planar $P_2N_4S_2$ ring, reported by Chivers and co-workers.²⁰ Figure 1 summarizes the structural arrangements of all chosen molecules.

The computations that constitute the basis for the results presented and discussed are based on density functional theory (DFT), and by now, a plethora of density functionals is available for electronic structure calculations. The reproduction of experimental results often serves as criterion to judge the

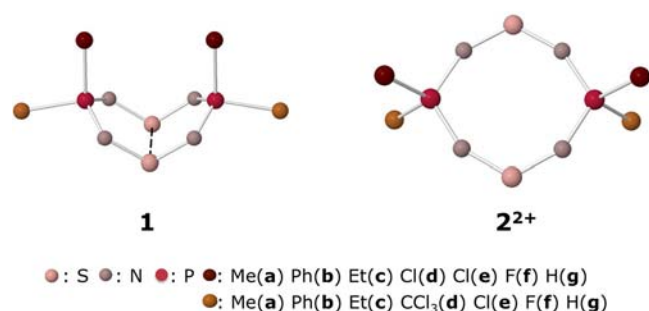


Figure 1. Geometric arrangements of folded diphosphadithiatetrazocines **1a–1g** and of their planar cationic counterparts **2a²⁺–2g²⁺**.

performance and applicability of a chosen functional, and we thus begin with a brief discussion of optimized diphosphadithiatetrazocine minimum geometries.

The Cross-Ring Sulfur–Sulfur Separation. The first structural determination of diphosphadithiatetrazocine systems by DFT revealed important methodological aspects:²¹ Hyper-GGAs, chosen from the fourth rank of Jacob’s ladder of density functional approximations,²² in combination with extended basis sets are a suitable choice for describing neutral $R_2P(NSN)_2PR_2$ molecules. But B3LYP is no synonym for DFT,²³ and in the current work, the relevant geometries are based on Becke’s original hybrid-formulation B3PW91²⁴ in combination with a balanced triple- ζ basis (def2-TZVP).²⁵

The putative sulfur–sulfur bond is at the center of the present work and values for the transannular $S\cdots S$ separation $d(S\cdots S)$ from current and previous computational work are collected in Table 1.

The data presented in Table 1 confirm the previous observation that a well-balanced basis set is crucial for the proper description of any sulfur–sulfur bond in diphosphadithiatetrazocines. Variation in basis set might cause a bond distance change in the range of 10–20 pm (compare entries 1 and 2, and entries 4 and 5). Furthermore, calculations that employ basis sets of comparable quality but utilize different hyper-GGAs might result in $d(S\cdots S)$ values that differ by about 10 pm (compare entries 1 and 3). Also included in Table 1 are $d(S\cdots S)$ data obtained from crystal structure determinations. The computational approach chosen for the production runs of the current contribution produces sulfur–sulfur separations that are in fine agreement with experiment (compare entries 1 and 3), which establishes a trustworthy basis for further analyses.

The Strength of the Cross-Ring Sulfur–Sulfur Interaction. To decide whether two atoms are bonded or not, a first orbital inspection provides arguments that are familiar to most chemists. Molecule **1a** exhibits a frontier orbital picture —

presented in Figure 2 — that is typical for folded diphosphadithiatetrazocines, and the appearance of the highest

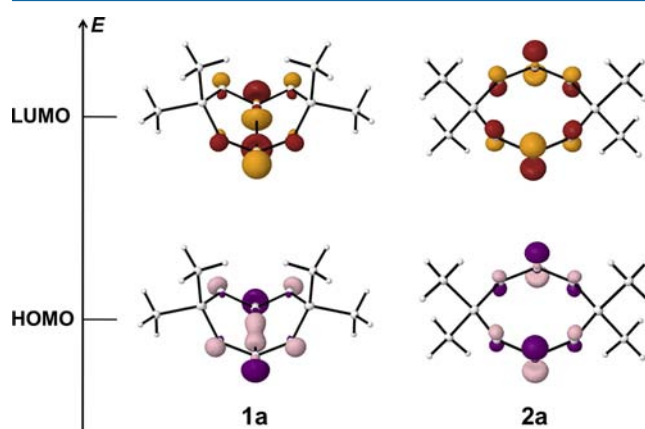


Figure 2. Kohn–Sham frontier molecular orbitals for **1a** and **2a** (contour value: 0.10 au).

occupied Kohn–Sham molecular orbital makes a strong case for the existence of a cross-ring $S\cdots S$ bond.

This observation seems to open up the possibility to determine the strength of the $S\cdots S$ interaction BE_{SS} : dicationic ground state geometries **2²⁺** serve as basis for planar, but neutral diphosphadithiatetrazocines **2**, and the isomerization energy for the process $2 \rightarrow 1$ is assumed to be directly related to BE_{SS} . The energy of this reaction is referred to as folding energy ΔE_{fold} and to a first approximation, the relationship $BE_{SS} \approx -\Delta E_{fold}$ holds. This reaction, among others that might be employed to determine a value of BE_{SS} , is illustrated in Figure 3, while Table 2 contains isomerization energies ΔE_{fold} relevant counterpoise corrected²⁶ reaction energies ΔE_{1S} , ΔE_{2S} , and strengths of the $S\cdots S$ interaction BE_{SS} .

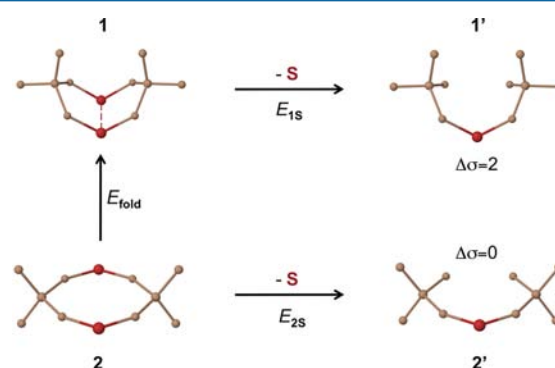


Figure 3. Elementary reactions for BE_{SS} determination.

Table 1. Transannular Sulfur–Sulfur Separation (in pm) for Diphosphadithiatetrazocines **1a–1g** in Their Folded Arrangement, Obtained from Computation (entries 1–5) and Experiment (entry 6)

			1a	1b	1c	1d	1e	1f	1g
$d(S\cdots S)$	1	B3PW91/def2-TZVP ^a	253	253	253	253	253	256	256
	2	B3PW91/TZVP ^a	267	262	263	264	265	269	269
	3	B3LYP/6-311+G(3df) ^b	262			262	263	267	
	4	B3LYP/6-31+G(3df) ^c							267
	5	B3LYP/6-31+G(d) ^c				279			287
	6	crystal Structure	255 ^d	253 ^e	250 ^f	253 ^f			

^aThis work. ^bRef 6. ^cRef 21. ^dRef 4. ^eRef 8. ^fRef 9.

Table 2. Reaction Energies ΔE_{fold} , ΔE_{1S} , ΔE_{2S} , and Strengths of S...S Interactions BE_{SS} for Diphosphadithiatetrazocines Representatives a–g^a

	a	b	c	d	e	f	g
ΔE_{fold}	-194	-206	-191	-204	-217	-200	-169
ΔE_{1S}	851	847	850	844	836	858	845
ΔE_{2S}	702	705	698	708	708	751	723
BE_{SS}	149	142	152	136	128	107	122

^aIn kJ/mol; see Figure 3 for reaction definitions.

While BE_{SS} -values derived from ΔE_{fold} result in a reasonable S–S bond energy (≈ 200 kJ/mol) that falls within the lower range of Denk's disulfide bond-strength scale (170–330 kJ/mol), specific aspects are in qualitative disagreement with previous work. The data of Table 2 indicate that halogen substitution in 1- and 5-position enhances the S–S bond strength, yet Chivers and co-workers have reported that the S...S interaction “is somewhat weaker in a 1,5-diphosphadithiatetrazocine with substituents of higher electronegativity”.⁶ It is most likely the neglect of changes in global homoaromaticity¹ associated with a folding process $1 \rightarrow 2$ that is to a large part responsible for this discrepancy.

In a direct approach to cross-ring sulfur–sulfur bonding, sulfur removal energies are calculated. The energy for the reaction $1 \rightarrow 1' + S$ is referred to as ΔE_{1S} (see Figure 3). Basic orbital arguments suggest that the resulting fragment $1'$ has two unpaired electrons; we classify the electronic states resulting from spin-independent density calculations in terms of their spin density, $\Delta\sigma = |\rho(\beta) - \rho(\alpha)|$.

The bonding interaction of each sulfur atom in diphosphadithiatetrazocines is not restricted to the build-up of a cross-ring S...S link, but if one considers the same reaction for a planar ring system $2 \rightarrow 2' + S$ with a sulfur removal energy ΔE_{2S} , and if one further assumes that the individual bonding components for sulfur atoms, such as S–N bonds, are approximately the same in the isoelectronic and isomeric folded and planar systems 1 and 2 , one arrives at an estimate

for the strength of an S...S bond as $BE_{SS} = \Delta E_{1S} - \Delta E_{2S}$. Relevant energies are collected in Table 2.

The energies for a transannular sulfur–sulfur bond are now in agreement with previous results in that substituents at phosphorus reduce the S–S bond strength as their electronegativity increases. In general, electron-withdrawing substituents weaken, while electron-donating groups strengthen the cross-ring sulfur interaction.

The cross-ring S–S bond strength for **1a** has been estimated before using a similar fragment-based approach, but choosing an anionic rather a cationic model for a planar $P_2N_4S_2$ ring.²⁷ Given the fact that the previous analysis did not use optimized reference geometries, but estimated structures based on related solid-state arrangements^{4,28} – an approach that can be expected to slightly underestimate the sulfur–sulfur interaction energy – the previous value, $BE_{SS}(\mathbf{1a}) = 133$ kJ/mol, and the current result, $BE_{SS}(\mathbf{1a}) = 149$ kJ/mol, are in gratifying agreement.

Of foremost significance is the notion that BE_{SS} energies based on sulfur removal fall outside the range of disulfide bond energies established by Denk⁷ and are significantly smaller. The fragment-based analyses suggest that there is some stabilizing cross-ring S...S interaction within folded diphosphadithiatetrazocines, which however is not the same as a general disulfide bond. Topology analyses of electron densities might provide favorable insights into the essentials of transannular sulfur–sulfur bonding.

Topology of the Cross-Ring Sulfur–Sulfur Interaction.

To establish a frame of reference, we begin with a topology analysis of what might be considered a regular disulfide bond, and hydrogen disulfide **3** is chosen as a quintessential representative. The topologies of $\rho(\mathbf{r})$, the electron charge density, and of $\nu(\mathbf{r})$, a function based on electron local kinetic energy densities, are evaluated in terms of their (3,–3) and (3,–1) critical points (CPs). Since the concept of QCT is gaining more and more familiarity among chemists, we withhold a detailed description of the methodological background and refer the interested reader to the literature.^{15–17,29}

Topologies of $\rho(\mathbf{r})$ and $\nu(\mathbf{r})$ for compound **3**, and of $\nu(\mathbf{r})$ for compound **1a**, chosen as representative of folded diphospha-

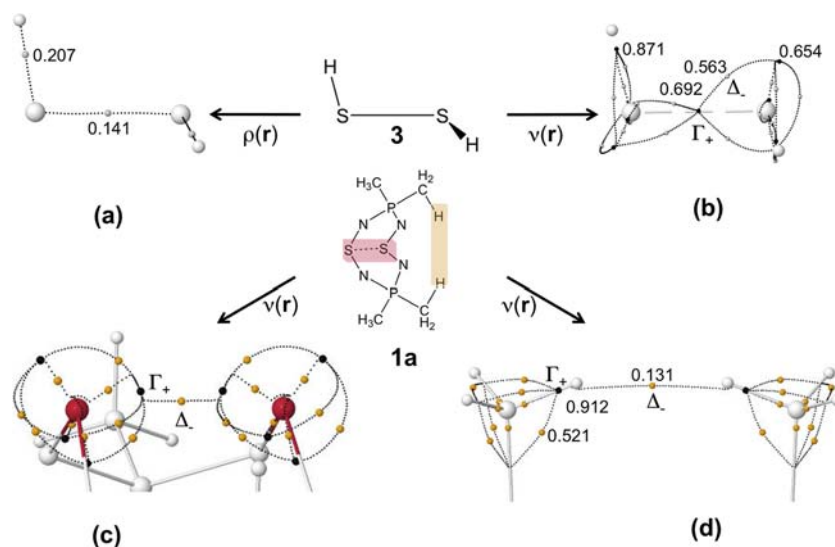


Figure 4. Density topologies of molecules **3** and **1a**: (a) (3,–1) CPs in $\rho(\mathbf{r})$ for **3**; (b) Γ_+ and Δ_- CPs in $\nu(\mathbf{r})$ for **3**; (c) Γ_+ and Δ_- CPs in $\nu(\mathbf{r})$ for the S...S region in **1a**; (d) Γ_+ and Δ_- CPs in $\nu(\mathbf{r})$ for the H...H region in **1a** ((3,–1) and Δ_- CPs as gray and/or orange spheres; Γ_+ CPs as black spheres; BPs and maxKCLs as black dotted lines).

Table 3. Selected $\nu(\mathbf{r})$ -Values of Two Critical Points Γ_+ and Δ_- for Diphosphadithiatetrazocines Representatives 1a–1g (see Figure 4)

	1a	1b	1c	1d	1e	1f	1g
ν_{Γ_+}	0.6134	0.6136	0.6137	0.6155	0.6142	0.6148	0.6123
ν_{Δ_-}	0.5381	0.5380	0.5396	0.5396	0.5349	0.5307	0.5293
$\Delta\nu$	0.0753	0.0756	0.0741	0.0759	0.0793	0.0841	0.0830

dithiatetrazocines, are depicted in Figure 4, and we have a first look at the charge density topology of H_2S_2 **3**. In general, the local maxima in $\rho(\mathbf{r})$ occur at the positions of the nuclei,²⁹ and the nuclear positions in $\rho(\mathbf{r})$ thus behave topologically as do (3,–3) CPs. The presence of (3,–1) CPs between each pair of nuclei, which are considered to be bonded to one another, completes the definition of a molecular structure. These critical points are thus referred to as bond critical points (BCP). Lines of maximum density that link neighboring nuclei of a molecular system in stable electrostatic equilibrium terminate at BCPs and establish an intermolecular connection. These lines project pathways of steepest descent and are referred to as bond paths (BP). All these features are well represented in the charge density topology of **3** (see Figure 4a); the charge value of 0.141 au for the BCP located between the two sulfur atoms is in adequate agreement with the results of a previous study.³⁰

Contrary to $\rho(\mathbf{r})$, the function $\nu(\mathbf{r})$ features additional (3,–3) CPs (attractors Γ_+) between connected atoms and in molecular regions associated with lone pairs.¹² Lines that trace a gradient path of steepest ascent originate at (3,–1) CPs (saddle points Δ_-) and terminate at attractors Γ_+ . Such lines are referred to as maximum kinetic connection lines (maxKCL). The $\nu(\mathbf{r})$ topology of **3** (see Figure 4b) suggests that the disulfide bond is not of pure covalent nature. For **3**, only a Γ_+ attractor is located approximately on the S–S connection line but no saddle points Δ_- . Thus, contrary to common covalent bonding,¹⁶ the interacting atoms are not directly connected to the bond attractor Γ_+ via maxKCL trajectories, which might be interpreted as the signature of a charge-shift bond.¹⁶

A charge-shift bond is dominated by the superposition of the covalent form and the two possible ionic forms of any bond between two atoms, and bonds bearing adjacent lone pairs and/or involving electronegative atoms are prone to charge-shift bonding.³¹ Thus, a charge-shift bond is not only variable in character but consequently also in energy. The fact that a disulfide bond is a charge-shift bond might provide a first explanation for Denk's extended sulfur–sulfur bond strength range.⁷

Chivers and co-workers have analyzed the charge density topology for a variety of diphosphadithiatetrazocines and localized BCPs that establish an S–S connection via bond paths. B3LYP/6-311+G(3df) charge densities at the S–S BCPs follow the order of **1a** (0.057 au) = **1d** (0.057 au) > **1e** (0.056 au) > **1f** (0.053 au).⁴ These values are significantly smaller than the one obtained for the disulfide bond in **3** by a factor of about 2.5 — in reasonable agreement with the observation that the average cross-ring sulfur–sulfur interaction is about half as strong as an average disulfide bond.

The authors also located additional BCPs between two hydrogen atoms or two chlorine atoms in **1a**, **1d**, or **1e**. But it is pointed out that their small $\rho(\mathbf{r})$ values of 0.007 au, 0.003 au, and 0.004 au, respectively, “demonstrate rather weak interactions”.⁶ After all, bond paths are not chemical bonds,³² and the interactions established by a topology analysis of the

charge density are not always fully comprehensible with chemical clairvoyance. Furthermore, within the framework of AIM, the question as to whether for a given molecule two atoms are bonded or not is only meaningful in the context of well-defined reference geometries,³³ and the search for bonds is strongly affected by the choice of the computational approach.³⁴

These observations might indicate that the theory of AIM has its rightful critics, and BPs and BCPs are not to be mistaken as indicators of a stabilizing interaction.³⁵ We would agree with the viewpoint that a model of the chemical bond should “possess predictive power”,³⁵ and the topology of $\nu(\mathbf{r})$ offers a more detailed description of bonding. We recall that $\nu(\mathbf{r})$ -values > 1/2 indicate stabilization and that the topology of $\nu(\mathbf{r})$ features an additional attractor Γ_+ between bonded atoms. For a covalent bond, we find at least one additional saddle point Δ_- located in close proximity of atomic connection line, with a $\nu(\mathbf{r})$ -value < 1/2 and establishing a direct connection between bond Γ_+ and atom Γ_+ .¹⁶ For a charge shift bond, we still see a bond attractor Γ_+ , but not in direct connection to the atomic centers. One might refer to these two types of bonds as primary electron-sharing bonds. Yet another situation is observed for the cross-ring sulfur–sulfur interactions in diphosphadithiatetrazocines, exemplified for **1a** in Figure 4c. No bond attractor is located between the sulfur atoms, but a (3,–1) saddle point Δ_- , in kinetic connection with lone pair attractors Γ_+ of the two sulfur atoms. For molecules **1a–1g**, values of $\nu(\mathbf{r})$ for these two critical points are collected in Table 3. We note that in all cases the Δ_- - $\nu(\mathbf{r})$ has a value > 1/2, but since the central point between the two sulfur atom has a lower $\nu(\mathbf{r})$ -value than the corresponding atomic connection points, the build-up of a kinetic connection line requires a destabilizing increase in kinetic energy. The resulting bond can be expected to be weaker than a bond centered on an attractor Γ_+ , and one might refer to such a bond as a secondary electron-sharing bond.

The fact that the topology of the kinetic energy density descriptor $\nu(\mathbf{r})$ depicts the cross-ring sulfur–sulfur bond as a weaker interaction than a regular disulfide bond is in qualitative agreement with our fragment based analysis. Since the two sulfur atoms are linked by a Δ_- -saddle point, it is not the $\nu(\mathbf{r})$ -value at the (3,–1) CP that directly correlates with our BE_{SS} estimates but the increase in the kinetic energy density required to establish a kinetic connection. The enlargement of the kinetic energy density correlates with a lessening of $\nu(\mathbf{r})$ -values, as represented by $\Delta\nu = \nu_{\Gamma_+}(\mathbf{r}) - \nu_{\Delta_-}(\mathbf{r})$. It can be expected that the smaller the destabilizing component $\Delta\nu$, the stronger the sulfur–sulfur bond, and simple linear regression establishes a correlation between these two bonding indicators. A regression plot $\text{BE}_{\text{SS}} = f(\Delta\nu)$ for compounds **1a–1g** based on data of Tables 2 and 3 is presented in Figure 5; the value for the coefficient of determination R^2 confirms a trustworthy relationship between these two approaches for bond description.

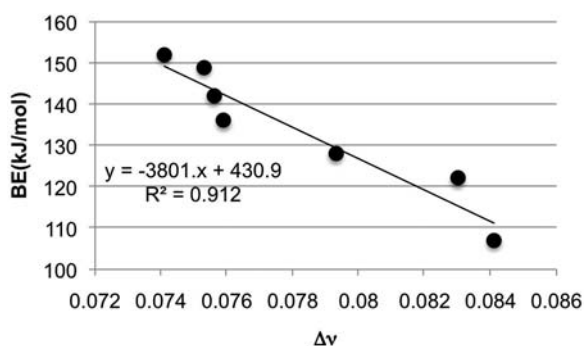


Figure 5. Linear regression plot $BE_{SS} = f(\Delta\nu)$ for compounds 1a–1g.

Not only does a topology analysis of the charge density $\rho(\mathbf{r})$ reveal the presence of (3,–1) CPs located between two H-atoms of methyl groups bonded to different P-atoms; the $\nu(\mathbf{r})$ topology displays similar features. In Figure 4d one observes how two adjacent hydrogen atoms are connected by maxKCLs, which originate at a saddle point Δ_- located between the two hydrogen centers. However, this is not an indication of a secondary electron-sharing bond. While the $\nu(\mathbf{r})$ value for the cross-ring S---S interaction is larger than 0.5 and indicates a stabilizing decrease in the local kinetic energy density, the $\nu(\mathbf{r})$ value for a putative hydrogen–hydrogen bond is significantly smaller than the reference value of the uniform electron gas. This is indicative for high-speed electrons and kinetic destabilization. While a kinetic connection exists between the two adjacent hydrogen atoms, this is not a stabilizing interaction, and the topology of $\nu(\mathbf{r})$ apparently does not support the idea of hydrogen–hydrogen bonding.

CONCLUSION

It appears that most important for the importance of being bonded is the importance of defining bonded. A fragment-based energy analysis allows one to associate a value for the S---S bond strength, which suggest that the sulfur atoms in diphosphadithiatetrazocines are bonded yet considerably weaker than in a common disulfide bond. But this picture of a cross-ring sulfur–sulfur bond is not free of ambiguities since it depends on the choice of fragments used to describe the formation and cannot directly be confirmed by experiment. The topology analysis of the charge density is experimentally accessible, albeit the relation between bond critical points and chemical bonding is not always easily established in a straightforward manner. The topology of a bond descriptor based on the local kinetic energy $\nu(\mathbf{r})$ provides a similar, but more detailed picture. (3,–3) maxima located between two bonded atoms are indicative of bonds that bear a strong covalent component, whereas (3,–1) saddle points with $\nu(\mathbf{r}) > 0.5$ indicate a weaker, secondary electron-sharing bond, as is the case for transannular S---S interactions. The change in local kinetic energy unifies the kinetic energy view of bonding with results obtained from fragment-based energy decomposition. While all these methods of analysis conclude that the sulfur atoms in diphosphadithiatetrazocines interact in a stabilizing fashion, the kinetic energy density description not only answers the question to the existence of a bond, but also provides some answers to the makeup of a bond.

As the first decade of the new millennium came to an end, Chivers and Kanu construed the state of affairs of one branch of chemical activity and offered an outlook into the future of main

group chemistry.³⁶ The authors identified areas of activity that range from fundamental to applied aspects, including novel aspects of chemical bonding. But disputes about the correct description of bonding, and in particular chemical bonding, are of a general nature and ongoing.³⁷ The local kinetic energy approach might outline a new direction to proceed beyond the bond.

COMPUTATIONAL DETAILS

Calculations based on the B3PW91 functional²⁴ that produced optimized geometries and final energies utilized the Gaussian 03 suite of programs.³⁸ If not noted otherwise, Gaussian 03 default values have been employed. Production runs made use of the balanced triple- ζ basis set with polarization def2-TZVP,²⁵ retrieved from the EMSL exchange library,³⁹ and comparison calculations were based on an older version of a polarized triple- ζ basis set TZVP,⁴⁰ as implemented in Gaussian 03.

Topological analyses of kinetic energy densities employed a suitably adjusted version of the program MORPHY,⁴¹ modified to allow for analytical evaluation of $\nu(\mathbf{r})$ and its derivatives, and for the use of Slater-type orbitals (STO). STO-based wave functions of polarized triple- ζ quality⁴² were generated by the computational chemistry package ADF.⁴³ Graphical representations of molecular frameworks and topology maps were produced using the graphical package Jmol.⁴⁴

ASSOCIATED CONTENT

Supporting Information

Optimized geometries, convergence criteria, frequencies, molecular total energies, as well as coordinates and values of $\nu(\mathbf{r})$ critical points. This material is available free of charge via the Internet at <http://pubs.acs.org>.

AUTHOR INFORMATION

Corresponding Author

*E-mail: jacobsen@kemkom.

Notes

The authors declare no competing financial interest.

ACKNOWLEDGMENTS

The Louisiana Optical Network Initiative (LONI) and the Modeling Laboratory for Nanostructures and Catalysis (MoLNaC) are gratefully acknowledged for granting access to their computational facilities.

REFERENCES

- (1) Rzepa, H. S. *Nat. Chem.* **2009**, *1*, 510–512.
- (2) Parr, R. G.; Ayers, P. W.; Nalewajski, R. F. *J. Phys. Chem. A* **2005**, *109*, 3957–3959.
- (3) Jacobsen, H. *Dalton Trans.* **2010**, *39*, 5426–5428.
- (4) Burford, N.; Chivers, T.; Codding, P. W.; Oakley, R. T. *Inorg. Chem.* **1982**, *21*, 982–986.
- (5) Zhang, Q.; Yue, S.; Lu, X.; Chen, Z.; Huang, R.; Zheng, L.; Schleyer, P. v. R. *J. Am. Chem. Soc.* **2009**, *131*, 9789–9799.
- (6) Chivers, T.; Hiltz, R. W.; Jin, P.; Chen, Z.; Lu, X. *Inorg. Chem.* **2010**, *49*, 3810–3815.
- (7) Denk, M. K. *Eur. J. Inorg. Chem.* **2009**, 1358–1368.
- (8) Burford, N.; Chivers, T.; Richardson, J. F. *Inorg. Chem.* **1982**, *22*, 1482–1487.
- (9) Chivers, T.; Edwards, M.; Parvez, M. *Inorg. Chem.* **1992**, *31*, 1861–1865.
- (10) Bitter, T.; Ruedenberg, K.; Schwarz, W. H. E. *J. Comput. Chem.* **2007**, *28*, 411–422. Ruedenberg, K.; Schmidt, M. W. *J. Comput. Chem.* **2007**, *28*, 391–410.
- (11) Schmider, H. L.; Becke, A. D. *J. Mol. Struct.—THEOCHEM* **2000**, *527*, 51–61.

- (12) Jacobsen, H. *Can. J. Chem.* **2008**, *86*, 695–702.
- (13) Jacobsen, H. *Dalton Trans.* **2009**, 4252–4258. Jacobsen, H. *Can. J. Chem.* **2009**, *87*, 965–973. Jacobsen, H. *Chem.–Eur. J.* **2010**, *16*, 976–987.
- (14) Yang, Y. *J. Phys. Chem. A* **2010**, *114*, 13257–13267. Steinmann, S. N.; Mo, Y.; Corminboeuf, C. *Phys. Chem. Chem. Phys.* **2011**, *13*, 20584–20592. Tai, T. B.; Tam, N. M.; Nguyen, M. T. *Chem. Phys. Lett.* **2012**, *530*, 71–76. Avaltroni, F.; Steinmann, S. N.; Corminboeuf, C. *Phys. Chem. Chem. Phys.* **2012**, *14*, 14842–14849. Tsipis, A. C. *Organometallics* **2012**, *31*, 7206–7212. Wang, J.-M.; Li, Z.-M.; Wang, Q.-R.; Tao, F.-G. *J. Mol. Mod.* **2013**, *19*, 83–95.
- (15) Popelier, P. L. A.; Brémond, E. A. G. *Int. J. Quantum Chem.* **2009**, *109*, 2542–2553.
- (16) Jacobsen, H. *Phys. Chem. Chem. Phys.* **2013**, *15*, 5057–5066.
- (17) Bader, R. F. W. *Atoms in Molecules: A Quantum Theory*; Oxford University Press: Oxford, 1990; Bader, R. F. W. *Chem. Rev.* **1991**, *91*, 893–928.
- (18) Jacobsen, H.; Ziegler, T. *Comments Inorg. Chem.* **1995**, *17*, 301–317.
- (19) Mitoraj, M. P.; Michalak, A.; Ziegler, T. *J. Chem. Theory Comput.* **2009**, *5*, 962–975.
- (20) Brock, M.; Chivers, T.; Parvez, M.; Vollmerhaus, R. *Inorg. Chem.* **1997**, *36*, 485–489.
- (21) Chung, G.; Lee, D. *Bull. Korean Chem. Soc.* **2000**, *21*, 300–304.
- (22) Perdew, J. P.; Ruzsinszky, A.; Tao, J.; Staroverov, V. N.; Suseria, G. E.; Csonka, G. I. *J. Chem. Phys.* **2005**, *123*, 062201.
- (23) Jacobsen, H.; Cavallo, L. In *Handbook of Computational Chemistry*; Leszczynski, J., Eds.; Springer: Heidelberg, 2012.
- (24) Becke, A. D. *J. Chem. Phys.* **1993**, *98*, 5648–5652.
- (25) Weigend, F.; Ahlrichs, R. *Phys. Chem. Chem. Phys.* **2005**, *7*, 3297–3305.
- (26) Boys, S. F.; Bernardi, F. *Mol. Phys.* **1970**, *19*, 553–566. Boys, S. F.; Bernardi, F. *Mol. Phys.* **2002**, *100*, 65–73.
- (27) Jacobsen, H.; Ziegler, T.; Chivers, T.; Vollmerhaus, R. *Can. J. Chem.* **1994**, *72*, 1582–1586.
- (28) Chivers, T.; Edwards, M.; Hilts, R. W.; Parvez, M.; Vollmerhaus, R. *J. Chem. Soc., Chem. Commun.* **1993**, 1483–1485.
- (29) Bader, R. F. W.; Nguyen-Dang, T. T.; Tal, Y. *Rep. Prog. Phys.* **1981**, *44*, 893–948.
- (30) Tang, T.-H.; Bader, R. F. W.; MacDougall, P. J. *Inorg. Chem.* **1985**, *24*, 2047–2053.
- (31) Hiberty, P. C.; Ramezani, R.; Song, L.; Wu, W.; Shaik, S. *Faraday Discuss.* **2007**, *135*, 261–272.
- (32) Bader, R. F. W. *J. Phys. Chem. A* **2009**, *113*, 10391–10396.
- (33) Jacobsen, H. *J. Comput. Chem.* **2009**, *30*, 1093–1102.
- (34) Jacobsen, H. *J. Phys. Chem. A* **2002**, *106*, 6189–6192.
- (35) Poater, J.; Solà, M.; Bickelhaupt, F. M. *Chem.–Eur. J.* **2006**, *12*, 2902–2905.
- (36) Chivers, T.; Konu, J. *Comment. Inorg. Chem.* **2009**, *30*, 131–176.
- (37) Ball, P. *Nature* **2011**, *469*, 26–28.
- (38) *Gaussian 03*, Revision D.02, Frisch, M. J. et al., Gaussian, Inc.: Wallingford, CT, 2004.
- (39) Schuchardt, K. L.; Didier, B. T.; Elsethagen, T.; Sun, L.; Gurumoorthi, V.; Chase, J.; Li, J.; Windus, T. L. *J. Chem. Inf. Model.* **2007**, *47*, 1045–1052.
- (40) Schäfer, A.; Huber, C.; Ahlrichs, R. *J. Chem. Phys.* **1994**, *100*, 5829–5835.
- (41) Popelier, P. L. A. *Comput. Phys. Commun.* **1996**, *93*, 212–240.
- (42) Van Lenthe, E.; Baerends, E. J. *J. Comput. Chem.* **2003**, *24*, 1142–1156.
- (43) te Velde, G.; Bickelhaupt, F. M.; van Gisbergen, S. J. A.; Fonseca Guerra, C.; Baerends, E. J.; Snijders, J. G.; Ziegler, T. *J. Comput. Chem.* **2001**, *22*, 931–967. Fonseca Guerra, C.; Snijders, J. G.; te Velde, G.; Baerends, E. J. *Theor. Chem. Acc.* **1998**, *99*, 391–403. ADF2008.01; S.C.M., *Theoretical Chemistry*; Vrije Universiteit: Amsterdam, The Netherlands; <http://www.scm.com> (accessed: 05-17-2013).
- (44) *Jmol: an open-source Java viewer for chemical structures in 3D*; <http://www.jmol.org/> (accessed: 05-07-2013).